J. C. S. Davie, P. D. Falloon, R. Kahana, R. Dankers, R. Betts, F. T. Portmann, D. B. Clark, A. Itoh, Y. Masaki, K. Nishina, B. Fekete, Z. Tessler, X. Liu, Q. Tang, S. Hagemann, T. Stacke, R. Pavlick, S. Schaphoff, S. N. Gosling, W. Franssen and N. Arnell: **Comparing projections of future changes in runoff and water resources from hydrological and ecosystem models in ISI-MIP,**

Earth System Dynamics Discussions, 2013

Supplementary Material

Supplementary Figure 1: Giorgi regions used in this study, after Ruosteenoja et al. (2002) and Giorgi and Bi (2005). ALA: Alaska and Western Canada; AMZ: Amazonia; ANT: Antarctic; ARC: Arctic; CAM: Central; America; CAN: Central North America; CAS: Central Asia; CGI: Canada, Greenland, Iceland; EAF: East Africa ; EAS: East Asia; ENA: Eastern North America; NAS: Northern Asia; NAU: Northern Australia; NEU: Northern Europe; SAF: South Africa; SAH: Sahara; SAS: South Asia; SAU: Southern Australia; SEA: Southeast Asia; SEU: Southern Europe and the Mediterranean; SSA: Southern South America; TIB: Tibetan Plateau; WAF: West Africa; WNA: Western North America

Supplementary Figure 2: Runoff change in individual model simulations, for 2070-2099 relative to 1981-2010. Hydrological models (a-g) are for the ISI-MIP “nosoc” setting, and ecosystems models (h-k) include changing CO_2 concentrations.

Supplementary Figure 3: Scatter plots of absolute present-day (1981-2010) precipitation against runoff change for 2070-2099 relative to 1981-2010, in the JULES simulations

Supplementary Figure 4: Changes in vegetation fractions in the JULES simulations with changing CO_2 concentrations, for 2070-2099 relative to 1981-2010

Supplementary Figure 5: Changes in vegetation fractions in the JULES simulations with fixed CO_2 concentrations, for 2070-2099 relative to 1981-2010

Supplementary Figure 6: The impact of vegetation change on runoff changes (mm/day) in the JULES simulations with a) changing CO2 concentrations, and b) fixed CO2, calculated as the difference in runoff change (2070-2099 minus 1981-2010) between simulations with dynamic and fixed vegetation.

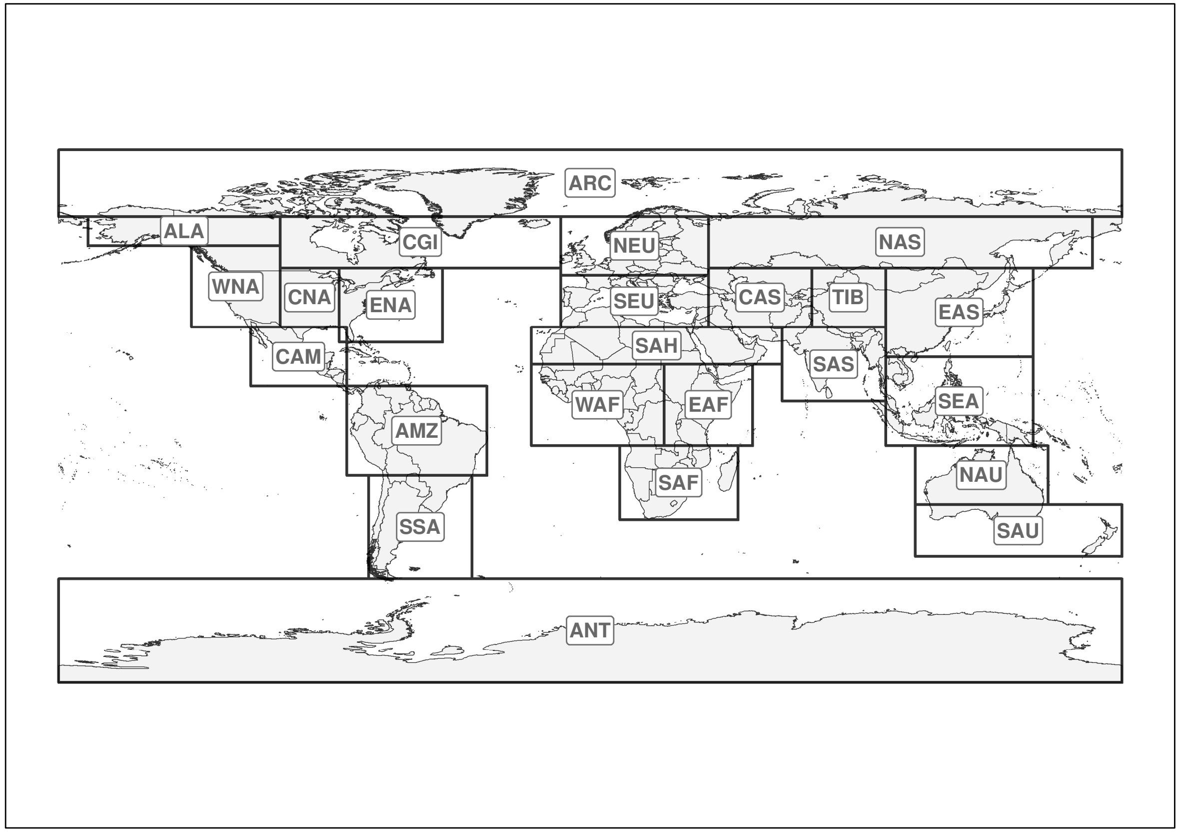

Supplementary Figure 1: Giorgi regions used in this study, after Ruosteenoja et al. (2002) and Giorgi and Bi (2005). ALA: Alaska and Western Canada; AMZ: Amazonia; ANT: Antarctic; ARC: Arctic; CAM: Central; America; CAN: Central North America; CAS: Central Asia; CGI: Canada, Greenland, Iceland; EAF: East Africa ; EAS: East Asia; ENA: Eastern North America; NAS: Northern Asia; NAU: Northern Australia; NEU: Northern Europe; SAF: South Africa; SAH: Sahara; SAS: South Asia; SAU: Southern Australia; SEA: Southeast Asia; SEU: Southern Europe and the Mediterranean; SSA: Southern South America; TIB: Tibetan Plateau; WAF: West Africa; WNA: Western North America

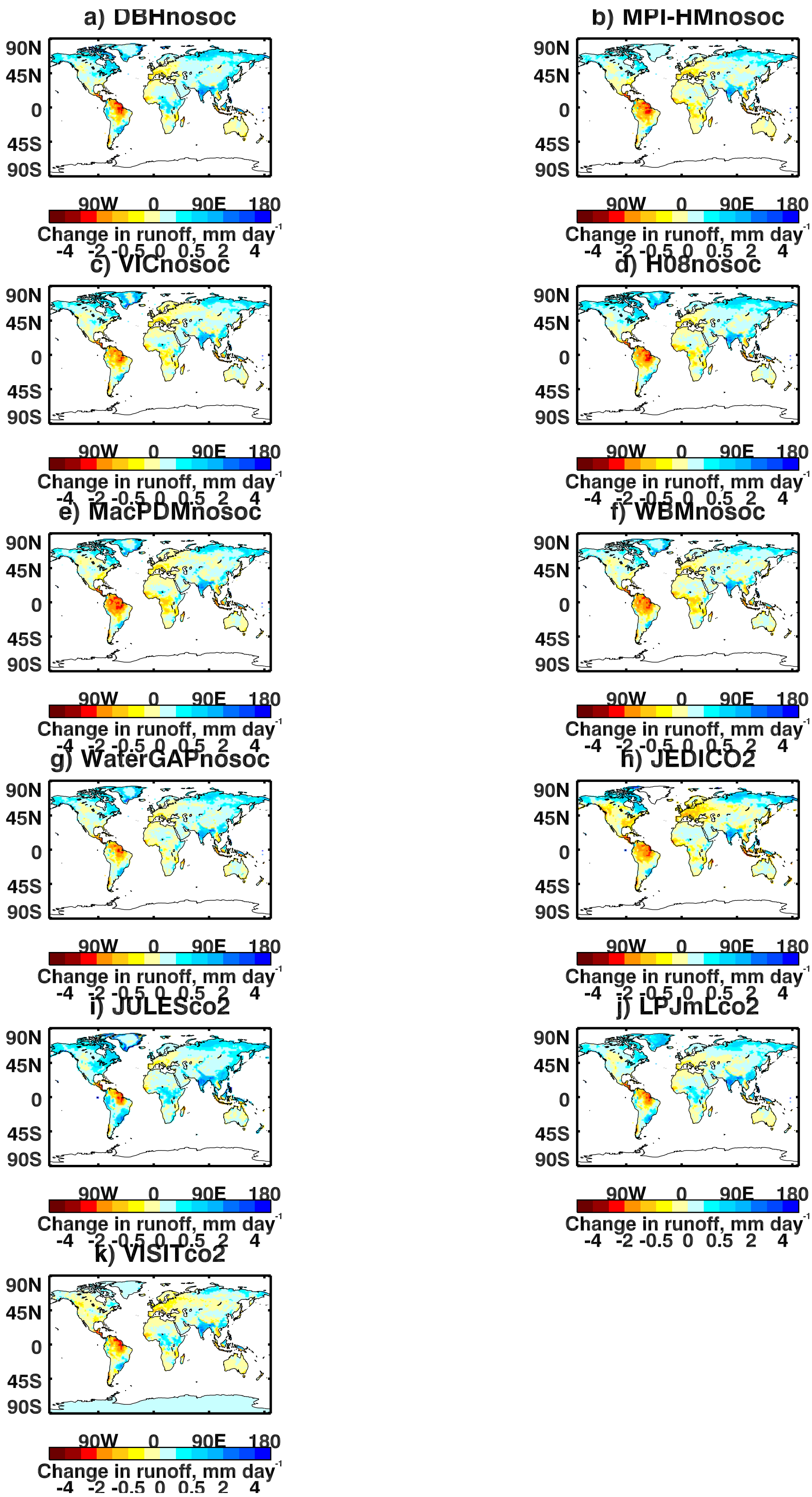

Supplementary Figure 2: Runoff change in individual model simulations, for 2070-2099 relative to 1981-2010. Hydrological models (a-g) are for the ISI-MIP "nosoc" setting, and ecosystems models (h-k) include changing CO_2 concentrations.

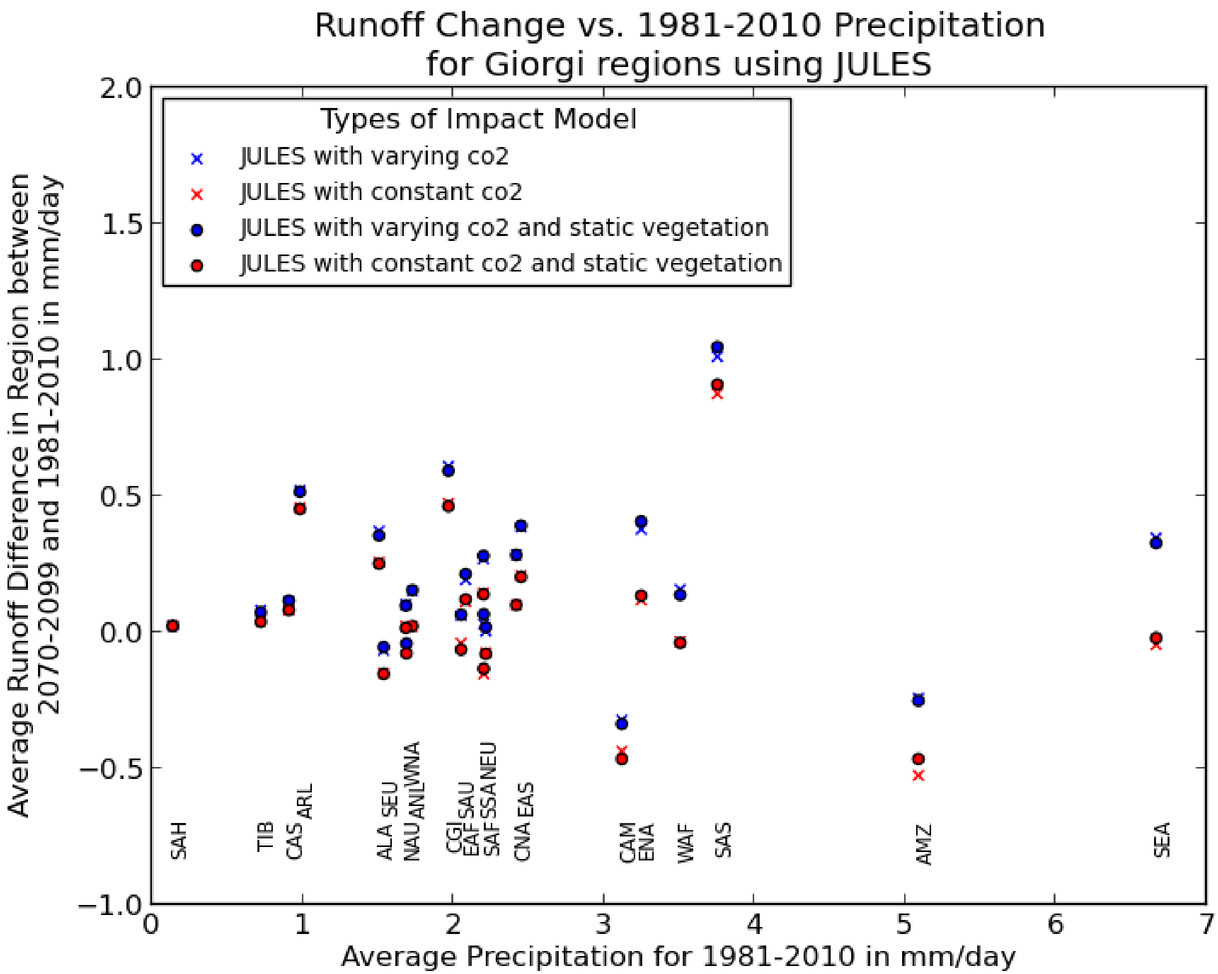

Supplementary Figure 3: Scatter plots of absolute present-day (1981-2010) precipitation against runoff change for 2070-2099 relative to 1981-2010, in the JULES simulations

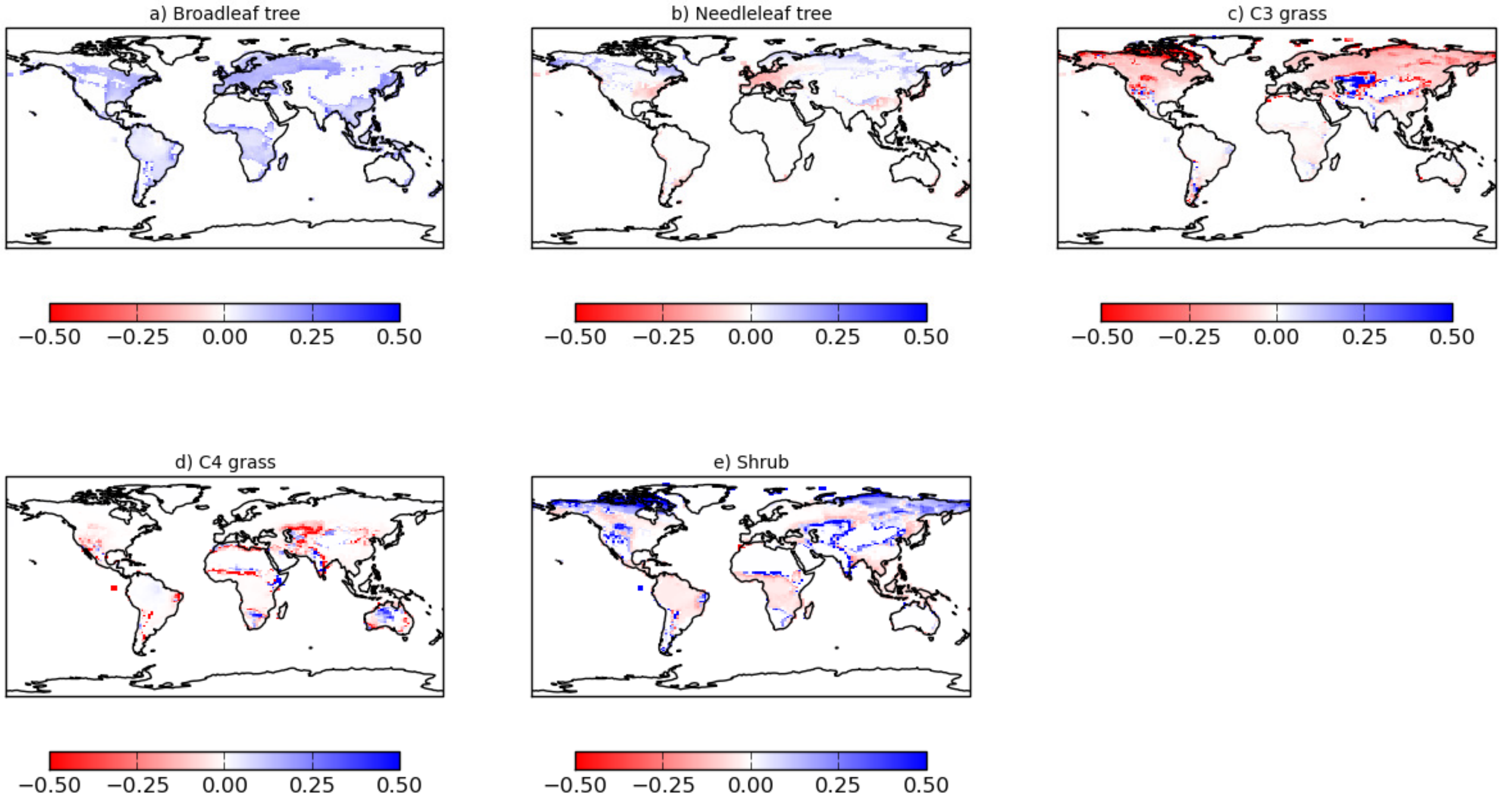

Supplementary Figure 4: Changes in vegetation fractions in the JULES simulations with changing CO_2 concentrations, for 2070-2099 relative to 1981-2010

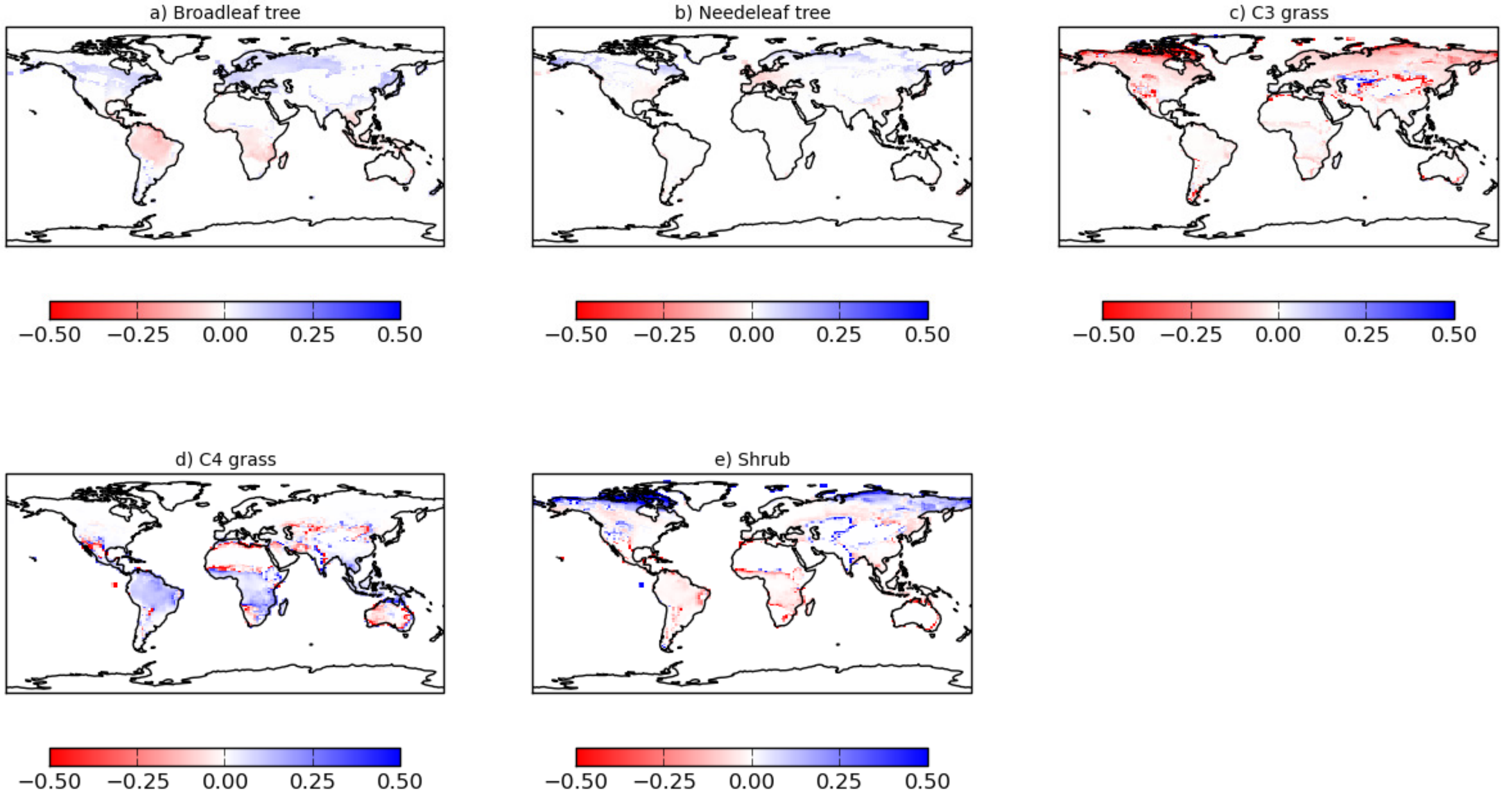

Supplementary Figure 5: Changes in vegetation fractions in the JULES simulations with fixed CO_2 concentrations, for 2070-2099 relative to 1981-2010

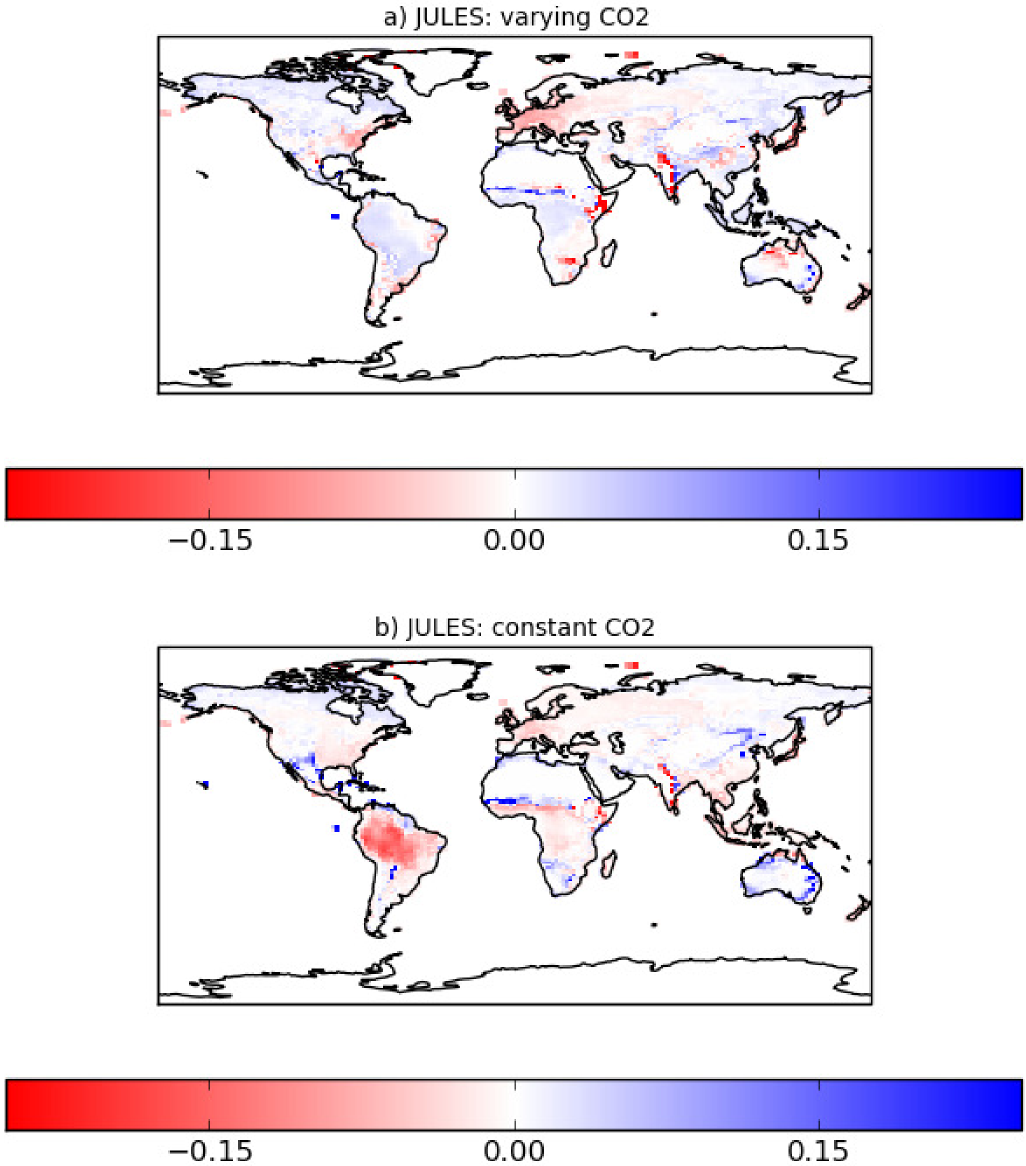

Supplementary Figure 6: The impact of vegetation change on runoff changes (mm/day) in the JULES simulations with a) changing CO2 concentrations, and b) fixed CO2, calculated as the difference in runoff change (2070-2099 minus 1981-2010) between simulations with dynamic and fixed vegetation.